ELSEVIER

Biophysical Chemistry 115 (2005) 37–47

Biophysical Chemistry

http://www.elsevier.com/locate/biophyschem

Phase synchronization and coherence resonance of stochastic calcium oscillations in coupled hepatocytes

Dan Wu, Ya Jia*, Lijian Yang, Quan Liu, Xuan Zhan

Department of Physics and Institute of Biophysics, Central China Normal University, Wuhan 430079, Hubei, China

Received 18 November 2004; received in revised form 25 December 2004; accepted 29 December 2004
Available online 19 January 2005

Abstract

The frequency of free cytosolic calcium concentration ($[Ca^{2+}]$) oscillations elicited by a given agonist concentration differs between individual hepatocytes. However, in multicellular systems of rat hepatocytes and even in the intact liver, $[Ca^{2+}]$ oscillations are synchronized and highly coordinated. In this paper, we have investigated theoretically the effects of gap junction permeable to calcium and of the total Ca^{2+} channel number located on endoplasmic reticulum on intercellular synchronization. Figures of ratio between mean oscillating frequency of coupled cells describe visually the process of phase-locking. By virtue of a set of phase analysis, we can observe a gradual transition from synchronous behavior to nonsynchronous behavior. Furthermore, a signal-to-noise ratio in two dimensional parameter space (coupling strength-total Ca^{2+} channel number) has suggested that, coherence resonance will occur for appropriate noise and coupling.

Keywords: Coupling strength; Ca^{2+}; Channel number; Stochastic Ca^{2+} oscillations; Synchronization

1. Introduction

It is well known that biochemical oscillations are encountered at all levels of biological organization, with periods ranging from a fraction of a second to years [1]. Hormone-induced oscillations in intracellular Ca^{2+} concentration have important roles in the physiology of most cell types [2–5]. Isolated hepatocytes as well as many other cells, exhibit $[Ca^{2+}]$ oscillations upon stimulation with low concentrations of IP_3(inositol 1,4,5-triphosphate)-dependent agonists [6,7]. $[Ca^{2+}]$ oscillations in hepatocytes play important roles in regulation. For example, Ca^{2+} regulates phosphorylation–dephosphorylation cycle process involved in glycogen degradation, which have been investigated theoretically [8,9].

Intracellular wave-like propagation of $[Ca^{2+}]$ oscillations across single cells is driven mainly by a regenerative process of Ca^{2+} release from the endoplasmic reticulum, mediated by IP_3 receptors [5,10]. In the intact liver, Robbgaspers and Thomas [11] and Nathanson et al. [12] found that calcium oscillations evoked by IP_3-linked agonists are organized as coordinated periodic waves across whole liver lobules (some 500 cells). On the smaller scale of isolated hepatocyte couplets, this coordination manifests itself as near-synchrony of calcium oscillations in adjacent cells [13]. This coordination has been investigated on both experiments [13–15] and theoretics [16–19].

A first paper by Tjordmann et al. [13] studied multicellular systems of rat hepatocytes, and confirm that: first, gap junction coupling is necessary for the coordination of $[Ca^{2+}]$ oscillations between the different cells; second, the presence of hormone at each hepatocyte is required for cell–cell Ca^{2+} signal propagation; third, functional differences between adjacent connected hepatocytes could allow a "pacemaker-like" intercellular spread of Ca^{2+} waves. A subsequent paper by the same authors [14] continued these studies, combining single-cell studies with experiments on cell populations isolated from the peripheral (periportal) and central (perivenous) zones of the liver cell plate. They found

* Corresponding author. Tel.: +86 2762714728; fax: +86 2767866070.
E-mail addresses: wud@phy.ccnu.edu.cn (D. Wu), jiay@phy.ccnu.edu.cn (Y. Jia).

0301-4622/$ - see front matter © 2005 Elsevier B.V. All rights reserved.
doi:10.1016/j.bpc.2004.12.047

strong evidence that the sequential pattern of calcium responses to vasopressin in these multicellular rat hepatocytes systems was due to a gradient of cell sensitivity (from cell to cell) for the hormone. The first cell to respond had the greatest sensitivity to the global stimulus, while the last cell to respond had the least sensitivity. Such gradients may impose an orientation on calcium waves in liver cells and provide a "pacemaker-like" mechanism for regulating intercellular communication in the liver.

However, the factors coordinating individual [Ca^{2+}] oscillations between connected cells and propagating intercellular Ca^{2+} waves are not precisely known. Dupont et al. [16] studied a model based on junctional coupling of multiple hepatocytes which differ in their sensitivity to the hormonal stimulus. As a consequence of this difference, the intrinsic frequency of intracellular calcium oscillations also varies from cell to cell. These oscillations are coupled by an intercellular messenger, which could be either Ca^{2+} or IP_3. The model yield intercellular waves that were confirmed experimentally. The authors also presented experimental evidence that the degree of synchronization is greater for the first few spikes, in agreement with the prediction of their model.

An alternative model has been proposed by Höfer [17] to explain the experimental results obtained by Tjordmann et al. [13]. Höfer noted that this experiment revealed a rather large variability in oscillator frequency between adjacent cells, which he argued is likely to be of random nature. As a consequence he studied the possibility that this originates from random variations in the structural properties of cells (cell size, cell shape, or ER content). They also predicted that synchronization of calcium oscillations in heterogeneous cells will occur in a window of coupling strength γ between 0.04 s^{-1} and 0.2 s^{-1}. In addition, Ca^{2+} was assumed to be the messenger passing through gap junctions. His results were in reasonable agreement with results in [13].

To obtain a better explanation of the experimental results, Gracheva et al. [18] have studied stochastic versions of the above two models. Their simulation is based on a Monte Carlo method. They found that, both stochastic models exhibit baseline fluctuations and variations in the peak heights of [Ca^{2+}], and that, for one model there is a distribution of latency times which is comparable to the experimental observation of spike widths.

Basing on Höfer's model and considering that the opening and closing of one gate in each IP_3 receptor is much slower than those of the other two gates [20], we employed Li–Rinzel model to describe the receptor flux of internal store [19]. In that paper, we have investigated theoretically the gap junction permeable to calcium and to IP_3 on intercellular synchronization by means of a mathematical model, respectively. It is shown that gap junction permeable to calcium and to IP_3 are effective on synchronizing calcium oscillations in coupled hepatocytes. Our theoretical results are similar either for the case of Ca^{2+} acting as coordinating messenger or for the case of IP_3 as coordinating messenger. There exists an optimal coupling strength for a pair of connected hepatocytes. Appropriate coupling strength and IP_3 level can induce various harmonic-locking of intercellular [Ca^{2+}] oscillations. Furthermore, a phase diagram in two dimensional parameter space of the coupling strength and IP_3 level (or the velocity of IP_3 synthesis) has been predicted, in which the synchronization region is similar to Arnold tongue.

Although the above models are relatively successful, they have limitations. For example, the calcium spikes in [16] models are extremely sharp, whereas the experimental spikes are broader. Höfer's model predicts more reasonable spike widths, but predicts an intercellular synchronization at low stimulus that seems inconsistent with experiment in [18]. Höfer [17] assumed that three gates of each IP_3 receptor are in a quasi-steady state. In addition, the effects of intracellular IP_3 level and of gap junction permeable to IP_3 on the synchronization have not been studied. Although our recent work [19] has investigated those effects, it has only studied the deterministic dynamics of Ca^{2+} in coupled hepatocytes. In the investigation of stochastic effects of intercellular calcium wave propagation, [18] seems to pay little attention to the effects of different noise strength.

Stochastic models of intracellular Ca^{2+} spiking for a variety of cell types have been studied previously [21–23]. Our simulation bases on Höfer's model and employs stochastic Li–Rinzel model to describe the receptor flux, we have explored the phase synchronization and coherence resonance of stochastic calcium oscillations in coupled hepatocytes. The stochastic model used in this paper is based on Langevin method [24].

Firstly, we explore theoretically the effects of gap junction permeable to Ca^{2+} on the synchronization of two and three coupled cells. Secondly, the paper analyze the relationship between the ratio of mean oscillating frequency in coupled cells and the coupling strength or Ca^{2+} channel number. From the view of physics, two kinds of phase definitions are applied to characterize the synchronization, both of which afford a visual transformation from unsynchronized state to synchronized one. Finally, signal-to-noise ratio in two parameters space (coupling strength-total Ca^{2+} channel number) suggests that there exists coherence resonance for two or three coupled hepatocytes.

2. Model

Hormone-evoked calcium dynamics in hepatocytes (as in many other cell types) involve the interplay of calcium fluxes from and into the ER and across the plasma membrane, and possibly also other compartments such as mitochondria. We aim to analyze the dynamics of coupled cells, so a relatively simple model proposed by Höfer [17] is applied in this paper. Höfer's model involves: calcium

release fluxes from the ER (denoted by J_{rel}), calcium reuptake through the sarco/endoplasmic reticulum calcium ATPase (SERCA) (denoted by J_{SERCA}), the calcium fluxes across the plasma membrane (denoted by J_{in} and J_{out}), and the gap-junctional flux. Assuming spatial uniformity of the calcium concentration in the cytoplasm and the ER, the balance equations for the concentration of cytoplasmic-free calcium and the free calcium content of the whole cell in the ith cell (x_i and z_i, respectively) are given by:

$$\frac{dx_i}{dt} = \rho\left(\left(J_{in} - J_{out}\right) + \alpha\left(J_{rel} - J_{SERCA}\right)\right) + \gamma\left(x_j - x_i\right), \tag{1}$$

$$\frac{dz_i}{dt} = \rho\left(J_{in} - J_{out}\right) + \gamma\left(x_j - x_i\right), \tag{2}$$

the index i, j=1, 2. When more than two cells are studied, the last term in Eqs. (1) and (2) is replaced by $\gamma(x_{j+1}+x_{j-1}-2x_j)$. A conservation of the total cellular Ca^{2+} implies the constraint: $z=x+\beta y$. y denotes the free calcium concentration in the ER. ρ, α and β are structural characteristics of cell. γ is the junctional coupling strength. If taking γ=0, Eqs. (1) and (2) describe the dynamical behavior of isolated cells.

The expressions for these fluxes are:

$$J_{in} = v_0 + v_c\frac{P}{K_0 + P}, \tag{3}$$

$$J_{out} = v_4\frac{x^2}{K_4^2 + x^2}, \tag{4}$$

$$J_{SERCA} = v_3\frac{x^2}{K_3^2 + x^2}, \tag{5}$$

$$J_{rel} = \left(k_1 m_\infty^3 n_\infty^3 h^3 + K_2\right)(y - x), \tag{6}$$

P denotes the intracellular IP_3 concentration. This model assumes that three equivalent and independent subunits are involved in conduction in an IP_3R. Each subunit has one IP_3 binding site (m gate), and two Ca^{2+} binding sites (one for activation (n gate), the other for inhibition (h gate)). Because the IP_3 binding is at lease 200 times faster than the Ca^{2+} activation binding, and the Ca^{2+} activation binding is at least 10 times faster than the Ca^{2+} inactivation binding and the change rate of $[Ca^{2+}]$ during oscillations, the fast variables m, n can be replaced by their quasi-equilibrium values m_∞ and n_∞ [20]:

$$m_\infty = \frac{P}{d_p + P},$$

$$n_\infty = \frac{x}{d_a + x},$$

Höfer's model assumed that h also to be in a quasi-steady state. However, the opening and closing of h gate in each IP_3 receptor is much slower than those of the other two gates. Moreover, Höfer's model describes the deterministic behavior averaged for a large number of Ca^{2+} channels. The random opening and closing of these channels introduces stochasticity into the calcium release mechanism. There are several ways (such as Markov method, Langevin approach) to simulate this stochastic scheme [25,26]. Langevin approach is applied in this paper. Therefore, the balance equation for h is given by [20,24]:

$$\frac{dh}{dt} = \alpha_h(1 - h) - \beta_h h + G_h(t), \tag{7}$$

with

$$\alpha_h = d_2\frac{P + d_1}{P + d_3},$$

$$\beta_h = x,$$

$$\langle G_h(t)G_h(t')\rangle = \frac{\alpha_h(1 - h) + \beta_h h}{N}\delta(t - t'), \tag{8}$$

α_h and β_h are opening rate and closing rate for h gates, respectively. N indicates the total number of IP_3R channels. We use a spatially homogeneous channel density inside cells, which is an approximation. Because channels are not very close on the ER membrane and show a tendency to cluster. Moreover, stochastic channel behavior and channel clustering are closely linked [23] due to huge gradients of the concentration of free Ca^{2+} [27]. However, the approximation of a spatially homogeneous cluster density is simple to manage numerically. Approximation of a spatially homogeneous cluster density is also applied in [28,29]. The values of these parameters [16,19] are: ρ=0:02 μm, α=2.0, β=0.1, v_0=0.2 μM s^{-1}, v_c=4.0 μM s^{-1}, v_3=9.0 μM s^{-1}, v_4=3.6 μM s^{-1}, k_1=40.0 s^{-1}, k_2=0.02 s^{-1}, K_0=4.0 μM, K_3=0.12 μM, K_4=0.12 μM, d_a=0.23 μM, d_p=1.66 μM, d_2=0.6 μM, d_1=0.3 μM, d_3=0.2 μM. To supply the demand of model, we have made a little change to parameters d_a, d_p and d_2. Parameter P is considered as a control parameter and is treated as a crucial free parameter.

To simulate the effects of the coupling strength and of other factors on the synchronization of intercellular Ca^{2+} oscillations in coupled hepatocytes, Eqs. (1), (2) and (7) were integrated by the forward Euler algorithm with a time step of 0.001 min. In each calculation, the time evolution of the system lasted 1000 min after transient behavior was discarded. The Gaussian noise sources are generated at each integration step by "Minimal" random number generator of Park and Miller with Bays-Durham shuffle and added safeguards [30].

3. Results

3.1. Comparison with experimental results

The calcium dynamics of isolated hepatocytes are well characterized experimentally. There exists a critical agonist dose above which a hepatocyte responds with regular calcium oscillations. The bifurcation diagrams for the intracellular Ca^{2+} concentration in an isolated hepatocyte are plotted in Fig. 1. The solid line is for deterministic case, which shows that, increase of IP_3 level gives rise to intracellular [Ca^{2+}] oscillations, and that at large agonist dose, oscillations disappear again via a second Hopf bifurcation and then the average cytosolic Ca^{2+} concentration is increased with the IP_3 stimulation level increasing. The dotted line and the dashed line are for stochastic case. The features of the deterministic bifurcation diagrams are well reproduced when the total number of channels is large (the dashed line: $N=10^6$). We can see that, the oscillation range in the stochastic case is larger than that one in the deterministic case, even if N is large. It can be concluded that, outside the range of intracellular [Ca^{2+}] oscillations for deterministic case, [Ca^{2+}] for stochastic case can also oscillate due to the random opening and closing of IP_3- and Ca^{2+}-gated channels.

To investigate the role of gap junction in synchronization of stochastic [Ca^{2+}] oscillations, we compare the evolution of x_1 and of x_2 after and before intercellular connection is blocked (Fig. 2). The different oscillating frequencies of [Ca^{2+}] in different cells in upper row (Fig. 2a and b) are caused by different hormone stimulus (P_1 and P_2 denote the intracellular IP_3 level in the two cells, respectively). While this difference in nether row is due to the different Ca^{2+} channel number (N_1 and N_2 denote the total IP_3R channel number in the two cells, respectively). When intercellular connection is blocked (Fig. 2a and c, $\gamma=0.01$ s^{-1}), the cells oscillate at their own intrinsic frequencies, and there is no fixed phase relation between the cells, which is consistent with the experimental results [7,31]. When gap junction recovers and coupling strength is big enough (Fig. 2b and d, $\gamma=0.15$ s^{-1}), the cells become synchronous. These results suggest that, whichever the cause for different intrinsic frequency is, gap junction is efficient and is required for the synchronization of hormone-induced cytosolic [Ca^{2+}] oscillations, which have been confirmed in [13,16–19]. In Fig. 2a, the intrinsic mean frequency of x_1 is about 0.008 s^{-1} and that one of x_2 is about 0.03 s^{-1}. When gap junction recovers, the mean frequency of [Ca^{2+}] oscillations for the two cells are both equal to 0.022 s^{-1}. One cell of the two coupled cells which oscillates quicker seems to impose its frequency on the other cell. This is consistent with the fact that, upon coupling of these individual oscillating units, the cell with the highest frequency of oscillation will act as a "pacemaker" for the other cells [13]. Stochastic [Ca^{2+}] oscillations in three connected cells have been drawn in Fig. 3, in which similar results can be obtained.

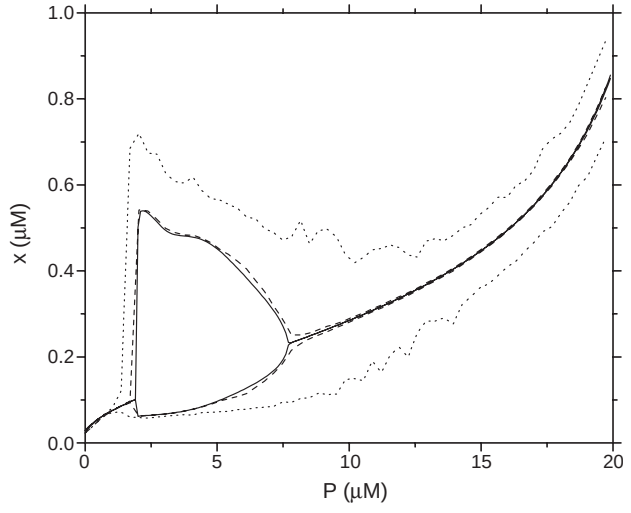

Fig. 1. The bifurcation diagrams of x in isolated hepatocytes are plotted against the stimulus parameter, P. (Solid line is for deterministic case; dotted line is for stochastic case (N=1000); dashed line is for stochastic case ($N=10^6$)). Within the range of P values giving rise to oscillations, both the maximum and the minimum of x in the course of oscillations are drawn.

In the experiment [13], the author first stimulated only one of the cells in the doublet with a hormone input (local perfusion). They then stimulated both cells simultaneously (global perfusion). From these studies they found that, local perfusion does not produce Ca^{2+} spiking in the second (unstimulated) cell, while global perfusion of both cells produces well-synchronized [Ca^{2+}] oscillations in the two cells. In Fig. 4a–c we show our results of stimulating only one cell in the doublet. It is found that the unstimulated cell (in which the IP_3 level is very low) can not show [Ca^{2+}] oscillations even if we increase the coupling strength to a big enough value ($\gamma=0.2$ s^{-1}). However, if we stimulate both hepatocytes, they respond with well-coordinated [Ca^{2+}] oscillations (see Fig. 2b). It can be concluded that sufficient IP_3 stimulus is necessary for the synchronization of stochastic [Ca^{2+}] oscillations in coupled hepatocytes [13,16,18,19].

What will occur when the IP_3 level in one of connected hepatocytes decreases suddenly? Fig. 5 depicts the case for three connected cells. When the IP_3 level in middle cell drops suddenly, the three connected cells which oscillated synchronously lose synchronization at the same time. When the IP_3 level recovers, synchronization of the three cells recover too and the first spike of the middle cell is very strong.

3.2. The frequency locking observed in coupled hepatocytes

To investigate the relationship of stochastic oscillations in coupled hepatocytes, the ratio of the mean oscillating frequencies of [Ca^{2+}] oscillation in two coupled cells has been drawn in Figs. 6 and 7. f_1 and f_2 denote the mean

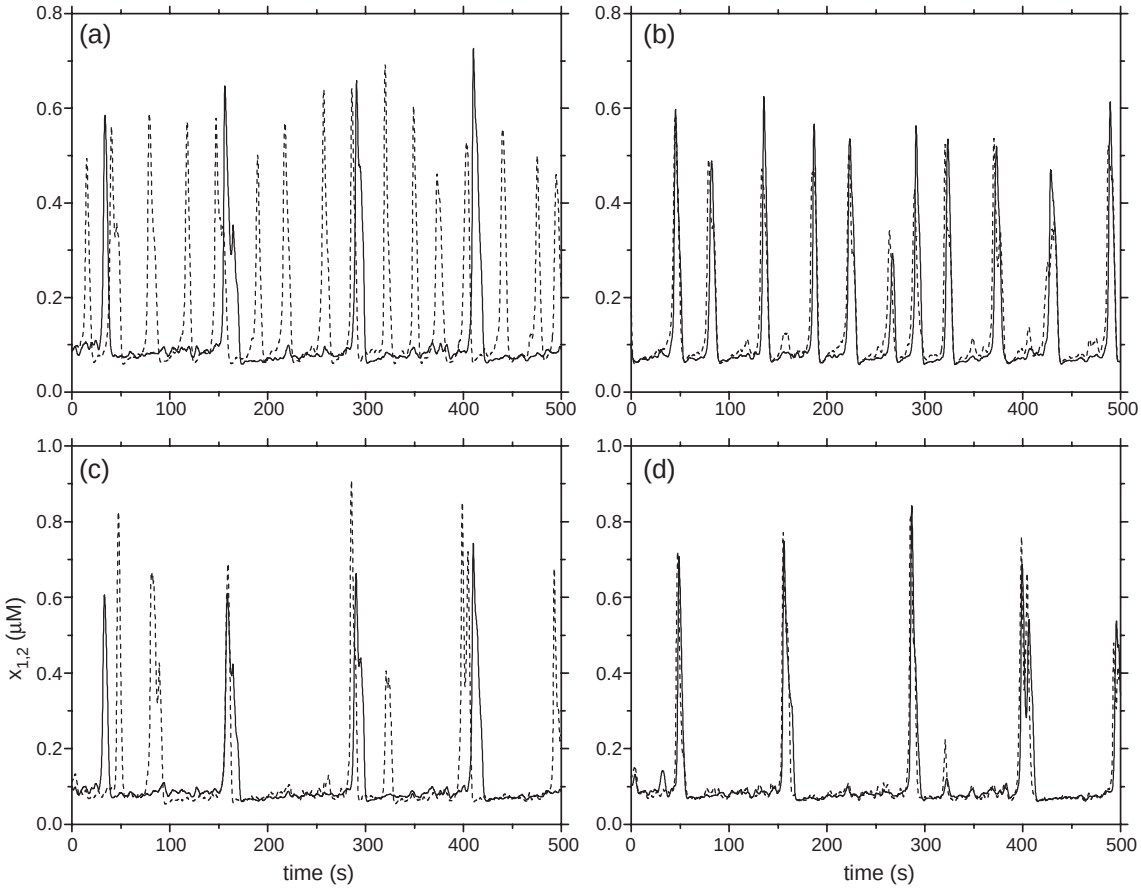

Fig. 2. Time courses of x_1 (solid line) and of x_2 (dashed line) in the stochastic version of Höfer's model. The parameter values for upper row are: P_1=1.5 μM, P_2=2.5 μM, N_1=N_2=500, (a) γ=0.01 s^{-1}; (b) γ=0.15 s^{-1}. The parameter values for nether row are: P_1=P_2=1.5 μM, N_1=500, N_2=100, (c) γ=0.01 s^{-1}; (d) γ=0.15 s^{-1}.

oscillating frequency of the [Ca^{2+}] oscillations during an equal long time for the two coupled cells, respectively.

Fig. 6a shows the f_1/f_2 rhythms as a function of the coupling strength for three different total Ca^{2+} channel number. The different intrinsic frequency of individual cells is due to the different IP_3 level (P_1=1.5 μM, P_2=2.5 μM). Fig. 6a reveals a steep sigmoidal nature of phase locking. When coupling strength γ is small, [Ca^{2+}] in the cell with P_1=1.5 μM oscillates rarely. Increasing the coupling strength further, the locking ratio gets closer to 1:1, and eventually the cells become synchronous, i.e. phase locking. With the noise increasing which is introduced by Ca^{2+} channel number, the sigmoidal nature become gentle. But there is still an obvious increase before the two cell become phase locking. In Fig. 6b, the different intrinsic frequency of individual cells is due to the different Ca^{2+} channel number (N_1=500, N_2=100). It can be seen that the steep sigmoidal nature only occurs at low IP_3 level.

In the following discussion, to highlight the effects of noise and coupling on connected cells, the IP_3 level is set at subthreshold value for deterministic case (P_1; P_2=1.5 μM, see solid line in Fig. 1). Therefore, in the figures following, the [Ca^{2+}] oscillations are induced by noise.

Fig. 7 shows the f_1/f_2 rhythms as a function of the total Ca^{2+} channel number in one cell (which is denoted by 2) for three different coupling strength. While the noise which introduced by Ca^{2+} channel number in the second cell (N_2) is varied (N_1, P_1 and P_2 are fixed), the frequency-locked region is easily identified within a certain range of N_2. The frequency-locked interval tends to become broader as the coupling strength is increased.

The distributions of inter-spike interval (ISI) of [Ca^{2+}] in coupled cells is plotted for four different coupling strength γ in Fig. 8. From Fig. 8a–d, it is clearly seen how the distributions of ISI of two oscillators approach each other and become coincident at some value of γ. Moreover, the inter-spike interval of coupled cells is more concentrated than that of single cell (data not shown). Thus, it can be inferred that synchronization can also decrease the variance of inter-spike interval compared to the variance in the single isolated cell.

3.3. Phase analysis of coupled hepatocytes

The phase locking of coupled cells is considered as an event lasting for a finite time and is described by the diffusion of phase [32] or by the shape of the phase

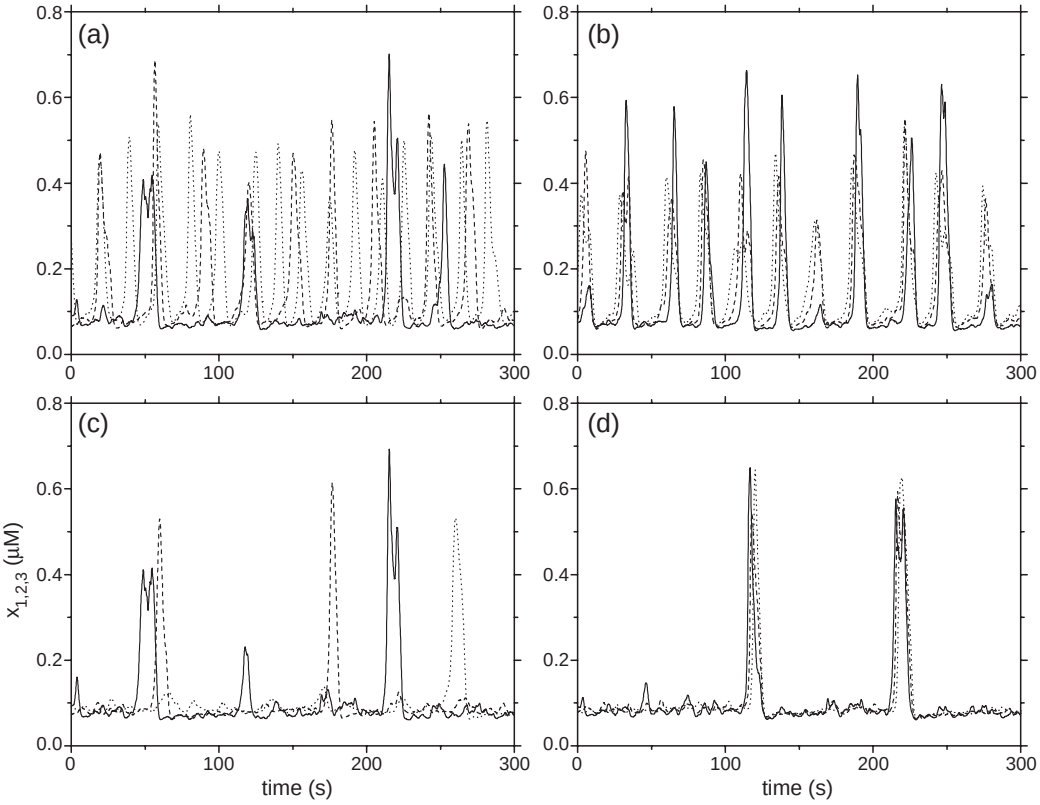

Fig. 3. Time courses of x_1 (solid line), of x_2 (dashed line) and of x_3 (dotted line) in the stochastic version of Höfer's model. The parameter values for upper row are: P_1=1.5 μM, P_2=2.5 μM, P_3=3.5 μM, N_1=N_2=N_3=500, (a) γ=0.01 s^{-1}; (b) γ=0.15 s^{-1}. The parameter values for nether row are: P_1=P_2=P_3=1.5 μM, N_1=100, N_2=500, N_3=1000, (c) γ=0.01 s^{-1}; (d) γ=0.15 s^{-1}.

difference distribution function [33]. To characterize the behavior in coupled cells, we introduce a phase [33] of the dynamics in each cell:

$$\phi_i(t) = 2\pi \frac{t - \tau_k^i}{\tau_{k+1}^i - \tau_k^i} + 2\pi k, \tag{9}$$

where τ_k^i is the time of the kth spike of the ith cell (in this paper, i=1, 2). Based on the phase variable for each cell, the instantaneous phase difference is defined as: $\Delta\phi$=ϕ_1−ϕ_2. We observe a transition from a regime, where the phases rotate with different velocities $\Delta\phi \sim \Delta\Omega t$($\Delta\Omega$=$|\langle\Delta\phi\rangle|$), to a synchronous state, where the phase difference does not grow with time $|\Delta\phi|$<const; $\Delta\Omega$=0. This transition is illustrated in Fig. 9.

We understand synchronization between two cells as the appearance of peaks in the distribution of the cyclic relative phase Φ=(ϕ_1−ϕ_2)mod2π [34]. Deviation of this distribution ($P(\Phi)$) from a uniform value characterizes the degree of synchronization. Therefore we have drawn Fig. 10, which illustrates the distribution function of the cyclic relative phase Φ (measured during a finite time) for three discernible

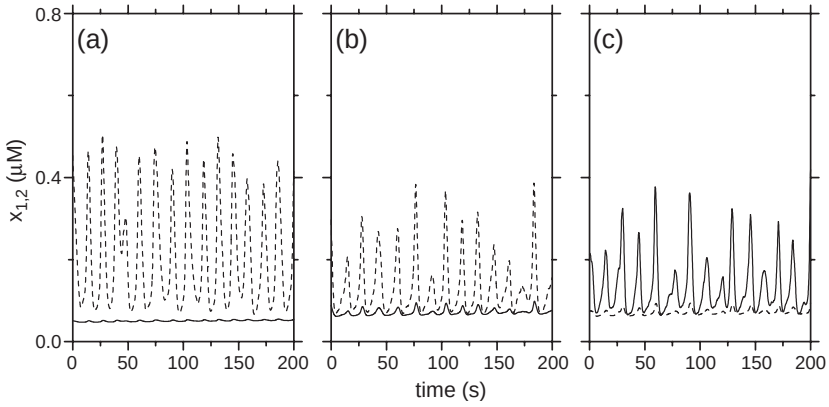

Fig. 4. Time courses of x_1 (solid line) and of x_2 (dashed line) at N_1=N_2=500. (a) P_1=0.5 μM, P_2=5.0 μM, γ=0.02 s^{-1}; (b) P_1=0.5 μM, P_2=5.0 μM, γ=0.2 s^{-1}; (c) P_1=5.0 μM, P_2=0.5 μM, γ=0.2 s^{-1}.

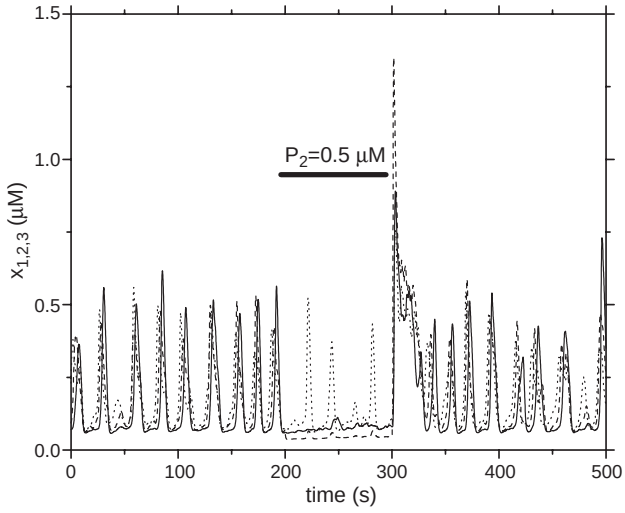

Fig. 5. Time courses of x_1 (solid line), of x_2 (dashed line) and of x_3 (dotted line) at P_1=2.0 μM, P_2=3.0 μM, P_3=4.0 μM, N_1=N_2=N_3=500 and γ=0.15 s^{-1}. An instantaneous drop of P_2 to a small value 0.5 μM just occurs at time=200 s. After 100 min, P_2 recover to 3.0 μM.

regimes (corresponding to those three phase difference in Fig. 9). For very weak coupling (Fig. 10c and f), the [Ca^{2+}] oscillations of each cell are essentially independent, because a noise-induced oscillations of one cell cannot excite its neighboring one. Due to the independent oscillations, the phase difference has a uniform random distribution on $(-2\pi, 2\pi)$. Whereas for a strong coupling strength (Fig. 10a and d), almost all cyclic relative phase concentrates on a

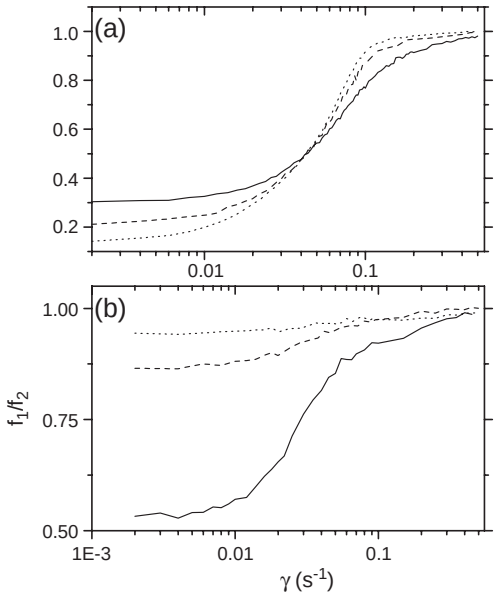

Fig. 6. (a) A ratio f_1=f_2 (where f_1 is the spike frequency of x_1 and f_2 is the spike frequency of x_2) as a function of coupling strength γ. P_1=1.5 μM, P_2=2.5 μM. solid line: N_1=N_2=200; dashed line: N_1=N_2=500; dotted line: N_1=N_2=1000. (b) A ratio f_1=f_2 (where f_1 is the spike frequency of x_1 and f_2 is the spike frequency of x_2) as a function of coupling strength γ. N_1=500 and N_2=100. solid line: P_1=P_2=1.5 μM; dashed line: P_1=P_2=2.5 μM; dotted line: P_1=P_2=5.0 μM.

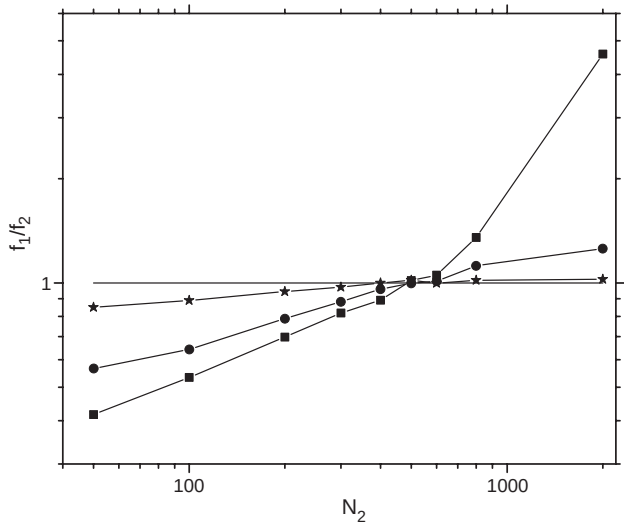

Fig. 7. A ratio f_1=f_2 (where f_1 is the spike frequency of x_1 and f_2 is the spike frequency of x_2) as a function of N_2 with P_1=P_2=1.5 μM, N_1=500. The coupling coefficient γ=0.07 s^{-1} (star), γ=0.02 s^{-1} (circle), γ=0.001 s^{-1} (square).

finite value near the zero, which corresponds to synchronization case.

3.4. Coherence resonance

From Fig. 7, it can be noted that the noise intensity (Ca^{2+} channel number N) plays the role of a control parameter governing the oscillating frequency in coupled cells. In this sense, the noise intensity acts like the nonlinearity and frequency parameter. To investigate the effect of frequency mismatch on the synchronization of coupled oscillators, we plot Figs. 11 and 12.

The quantity

$$s_i = \sin^2\left(\frac{\phi_i - \phi_{i+1}}{2}\right), \tag{10}$$

measures the phase synchronization effect of neighboring elements [35]. A spatiotemporal average of s_i, i.e.,

$$S = \lim_{T\to\infty}\frac{1}{T}\int_0^T \mathrm{d}t\left(\frac{1}{N}\sum_{i=1}^{N} s_i\right), \tag{11}$$

gives a measure of the degree of phase synchronization in the coupled system. For completely unsynchronized motion $S \approx 0.5$, while for globally synchronized system $S \approx 0$.

To measure the temporal coherence of the noise-induced motion, we examine the distribution of the pulse duration T_k=τ_{k+1}−τ_k. For a single element subject to noise, the distribution $P(T)$ has a peak at a certain value of T_k and an exponential tail at large values [36]. A measure of the sharpness of the distribution, for example,

$$R = \frac{\langle T_k\rangle}{\sqrt{\mathrm{Var}\ (T_k)}}, \tag{12}$$

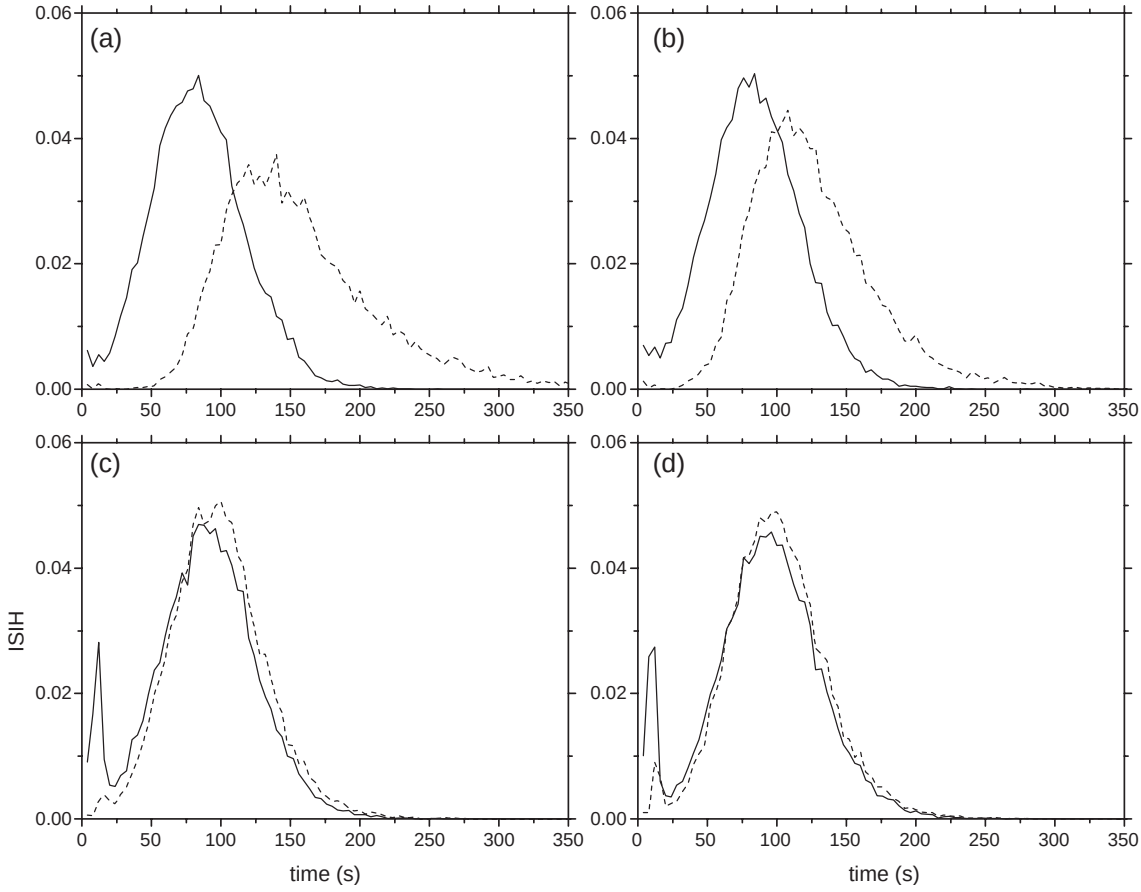

Fig. 8. The inter-spike interval histogram (ISIH) of x_1 (solid line) and of x_2 (dashed line) for different coupling strength γ. P_1=P_2=1.5 μM; N_1=100, N_2=500. (a) γ=0.001 s^{-1}; (b) γ=0.02 s^{-1}; (c) γ=0.07 s^{-1}; (d) γ=0.1 s^{-1}.

which can be viewed as signal-to-noise ratio, provides an indication of the coherence of the spike event. Biologically, this quantity is of importance because it is related to the timing precision of the information processing in some important systems [37]. For a single element, it has been shown that R possesses an optimal value at a certain level of noise [36]. Here we adopt the same measure coherence, with the distribution $P(T)$ constructed by pulse duration of all the N elements during a long enough period of time.

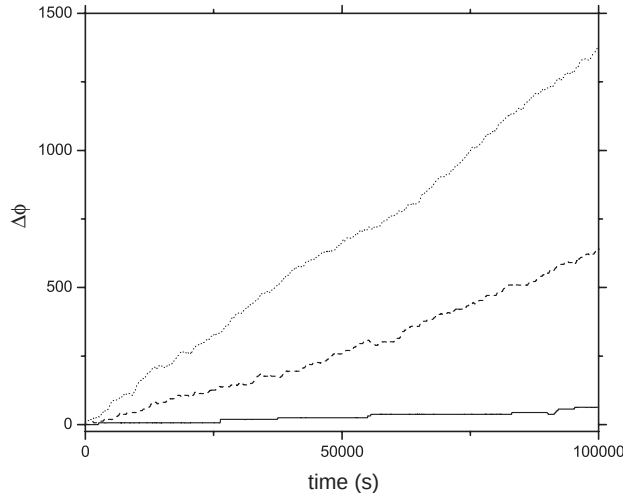

Fig. 9. The phase difference of the two coupled cells ($\Delta\phi$) as a function of time for γ=0.07 s^{-1} (solid line), γ=0.02 s^{-1} (dashed line), and γ=0.001 s^{-1} (dotted line), respectively. P_1=P_2=1.5 μM, N_1=500; N_2=1000.

R and S in the parameter space (γ, N) are shown for two and three coupled hepatocytes, respectively. From Fig. 11, we can observe that, for very weak coupling, $S \approx 0.5$, i.e., completely unsynchronized motion. However, $S \approx 0$ for strong coupling, i.e., synchronized system. This is in consistent with Fig. 10. In Fig. 12, for a fixed coupling strength γ, R increases first with noise level (small Ca^{2+} channel number corresponds to large noise), reaches a maximum, then decreases again, showing the typical resonant behavior without an external signal. In general, for a stronger coupling, a higher level of noise is needed to excite the system. Similarly, for a fixed noise level N, R increases with increasing γ until reaches an optimal value; after that, it decreases again.

4. Conclusions

In this article, basing on Höfer's model and employing stochastic Li–Rinzel model to describe the receptor flux, we have explore theoretically the intercellular Ca^{2+} oscillations

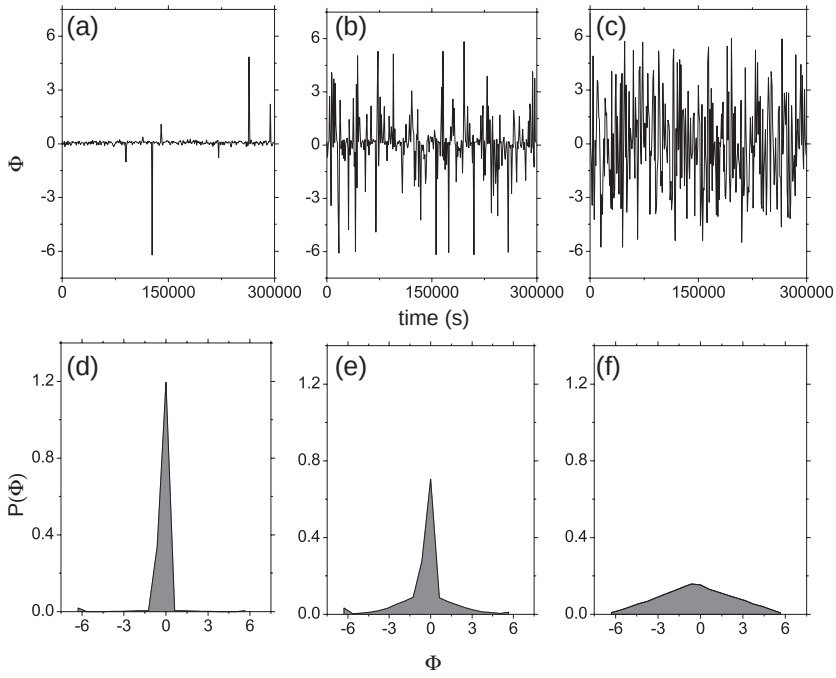

Fig. 10. The cyclic relative phase of the two coupled cells (Φ) as a function of time for (a) γ=0.07 s^{-1}, (b) γ=0.02 s^{-1}, and (c) γ=0.001 s^{-1}. Other parameters: P_1=P_2=1.5 μM, N_1=500; N_2=1000. (d–f) The corresponding distributions of the cyclic relative phase ((d) corresponding to (a); (e) corresponding to (b); (f) corresponding to (c)).

in coupled hepatocytes. Coupled hepatocytes are connected by gap junctions, which can be permeable to Ca^{2+}. The stochastic model in this paper are in better agreement with experiment than are the deterministic models.

By comparing bifurcation diagrams of isolated cell for deterministic case and for stochastic case (Fig. 1), it has been found that, the oscillation range for stochastic case is larger than that one for deterministic case even if Ca^{2+} channel number is very large, which is due to the random opening of closing of Ca^{2+} channel. In addition, the coherence between the deterministic bifurcation diagram and the stochastic one for large channel number confirms that, the application of the stochastic model in this paper is reasonable.

The frequency of [Ca^{2+}] oscillations elicited by a given agonist concentration differs between individual hepatocytes [7,31]. However, in multicellular systems of rat hepatocytes [38,39] and even in the intact liver [11,12], [Ca^{2+}] oscillations are synchronized and highly coordinated. This fact is well confirmed in our results. It has been also indicated that the coupled cells, in which their different

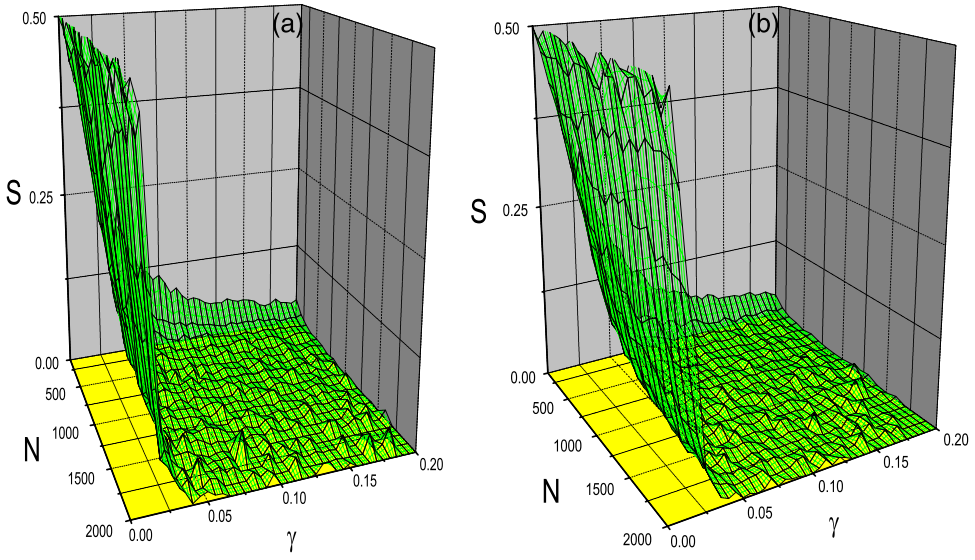

Fig. 11. Degree of phase synchronization S in the parameter space (γ–N) of connected hepatocytes. (a) Two connected cells: P_1=P_2=1.5 μM. (b) Three connected cells: P_1=P_2=P_3=1.5 μM.

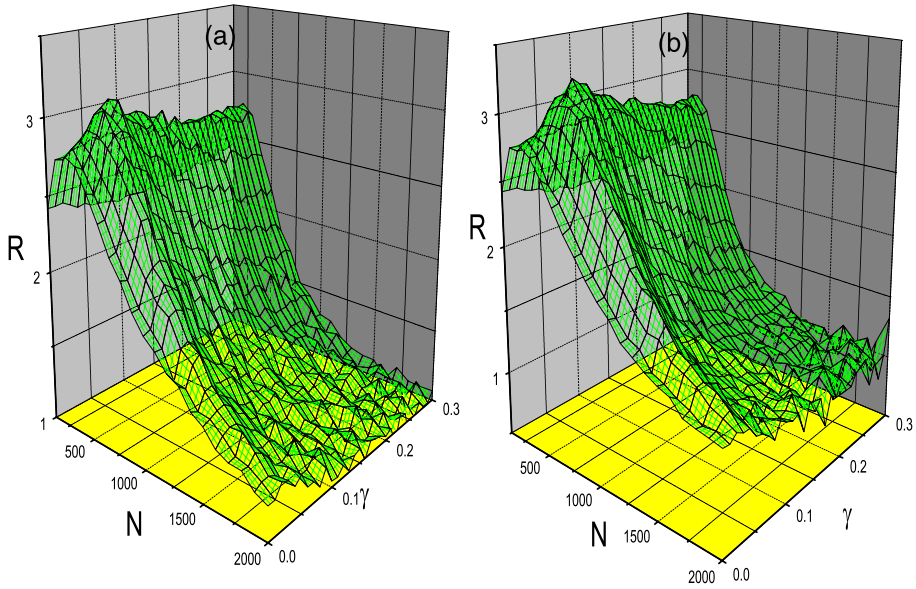

Fig. 12. Signal-to-noise ratio R in the parameter space ($\gamma - N$) of connected hepatocytes. (a) Two connected cells: $P_1=P_2=1.5$ μM. (b) Three connected cells: $P_1=P_2=P_3=1.5$ μM.

intrinsic oscillating frequencies are due to the different channel number, can become synchronous too.

A peculiar feature of intercellular Ca^{2+} waves in hepatocytes, compared with other cell types, is that they require the continuous presence of an agonist [13]. Both Figs. 4 and 5 demonstrate that sufficient and continuous IP_3 stimulus is necessary for the synchronization of stochastic [Ca^{2+}] oscillations in coupled hepatocytes.

The paper analyze the relationship between the ratio of mean oscillating frequency in coupled cells and the coupling strength or Ca^{2+} channel number. We observe that there is a steep sigmoidal nature of phase locking and the range of phase-locking relates to not only coupling strength but also Ca^{2+} channel number. Moreover, the evolution of inter-spike interval affords a visual transformation from unsynchronized state to synchronized one.

Furthermore, we introduce a phase definition to characterize the synchronization, which has not been used to analyze [Ca^{2+}] synchronization in hepatocytes as far as know. From Figs. 9 and 10, we can see not only the effects of coupling strength on phase difference and on relative phase distribution, but also a diversity of relative phase evolution.

The above analysis suggests that coupling strength and the Ca^{2+} channel number play important roles in the synchronization of [Ca^{2+}] oscillations in coupled hepatocytes. Therefore, we give a figure (Fig. 11) which describes the synchronous degree in these two parameters, which is in consistent with above results. Finally, signal-to-noise ratio in these two parameters suggests that coherence resonance occurs at appropriate number of Ca^{2+} channel. Therefore, we conclude that it is important to take into account stochastic effects in modelling calcium oscillations in connected hepatocytes.

Acknowledgments

This work was supported by the National Natural Science Foundation of China under Grant No. 10275026.

References

[1] A. Goldbeter, Biochemical oscillations and cellular rhythms. The Molecular Bases of Periodic and Chaotic Behaviour, Cambridge Univ. Press, Cambridge, 1996.
[2] M.J. Berridge, Inositol trisphosphate and calcium signalling, Nature 361 (1993) 315–325.
[3] O.H. Petersen, C.C.H. Petersen, H. Kasai, Calcium and hormone action, Annu. Rev. Physiol. 56 (1994) 297–319.
[4] T. Pozan, R. Rizzuto, P. Volpe, J. Meldolesi, Molecular and cellular physiology of intracellular calcium stores, Physiol. Rev. 74 (1994) 595–636.
[5] A.P. Thomas, G.S.J. Bird, G. Hajnoczky, L.D. Robbgaspers, J.W. Putney, Spatial and temporal aspects of cellular calcium signaling, FASEB J. 10 (1996) 1505–1517.
[6] N.M. Woods, K.S.R. Cuthberon, P.H. Cobbold, Repetitive transient rises in cytoplasmic free calcium in hormone-stimulated hepatocytes, Nature 319 (1986) 600–602.
[7] T.A. Rooney, E.J. Sass, A.P. Thomas, Characterization of cytosolic calcium oscillations induced by phenylephrine and vasopressin in single fura-2-loaded hepatocytes, J. Biol. Chem. 264 (1989) 17131–17141.
[8] D. Wu, Y. Jia, A. Rozi, Effects of inositol 1,4,5-trisphosphate receptor-mediated intracellular stochastic calcium oscillations on activation of glycogen phosphorylase, Biophys. Chemist. 110 (2004) 179–190.
[9] A. Rozi, Y. Jia, A theoretical study of effects of cytosolic Ca^{2+} oscillations on activation of glycogen phosphorylase, Biophys. Chemist. 106 (2003) 193–202.
[10] H. Kasai, O.H. Petersen, Spatial dynamics of second messengers: IP_3 cAMP as long-range and associative messengers, Trends Neurosci. 17 (1994) 95–101.

[11] L.D. Robbgaspers, A.P. Thomas, Coordination of Ca^{2+} signaling by intercellular propagation of Ca^{2+} waves in the intact liver, J. Biol. Chem. 270 (1995) 8102–8107.
[12] M.H. Nathanson, A.D. Burgstahler, A. Mennone, M.B. Fallon, C.B. Gonzalez, J.C. Sáez, Ca^{2+} waves are organized among hepatocytes in the intact organ, Am. J. Physiol. 32 (1995) G167–G171.
[13] T. Tordjmann, B. Berthon, M. Claret, L. Combettes, Coordinated intercellular calcium waves induced by noradrenaline in rat hepatocytes: dual control by gap junction permeability and agonist, EMBO J. 16 (1997) 5398–5407.
[14] T. Tordjmann, B. Berthon, E. Jacquemin, C. Clair, N. Stelly, G. Guillon, M. Claret, L. Combettes, Receptor-oriented intercellular waves evoked by vasopressin in rat hepatocytes, EMBO J. 17 (1998) 4695–4703.
[15] C. Clair, C. Chalumeau, T. Tordjmann, J. Poggioli, C. Erneux, G. Dupont, L. Combettes, Investigation of the roles of Ca^{2+} and $InsP_3$ diffusion in the coordination of Ca^{2+} signals between connected hepatocytes, J. Cell. Sci. 114 (2001) 1999–2007.
[16] G. Dupont, T. Tordjmann, C. Clair, S. Swillens, M. Claret, L. Combettes, Mechanism of receptor-oriented intercellular calcium wave propagation in hepatocytes, FASEB J. 14 (2000) 279–289.
[17] Th. Höfer, Model of intercellular calcium oscillations in hepatocytes: synchronization of heterogeneous cells, Biophys. J. 77 (1999) 1244–1256.
[18] M.E. Gracheva, R. Toral, J.D. Gunton, Stochastic effects in intercellular calcium spiking in hepatocytes, J. Theor. Biol. 212 (2001) 111–125.
[19] D. Wu, Y. Jia, X. Zhan, L.J. Yang, Q. Liu, Effects of gap junction to Ca^{2+} and to IP_3 on the synchronization of intercellular calcium oscillations in hepatocytes, Biophys. Chemist. 113 (2004) 145–154.
[20] Y. Li, J. Rinzel, Equations for $InsP_3$ receptor-mediated $[Ca^{2+}]_i$ oscillations derived from a detailed kinetic model: a Hodgkin–Huxley like formalism, J. Theor. Biol. 166 (1994) 461–473.
[21] J. Keizer, G.D. Smith, Spark-to-wave transition: salitatory transmission of calcium waves in cardiac myocytes, Biophys. Chemist. 72 (1998) 87–100.
[22] M. Falcke, Deterministic and stochastic models of intracellular Ca^{2+} waves, New J. Phys. 5 (2003) 96.1–96.28.
[23] M. Falcke, On the role of stochastic channel behavior in intracellular Ca^{2+} dynamics, Biophys. J. 84 (2003) 42–56.
[24] P. Jung, J.W. Shuai, Optimal sizes of ion channel clusters, Europhys. Lett. 56 (2001) 29–35.
[25] A.F. Strassberg, L.J. DeFelice, Limitations of the Hodgkin–Huxley formalism: effects of single channel kinetics on transmembrane voltage dynamics, Neural Comput. 5 (1993) 843–855.
[26] R.F. Fox, Y. Lu, Emergent collective behavior in large numbers of globally coupled independently stochastic ion channels, Phys. Rev., E 49 (1994) 3421–3431.
[27] R. Thul, M. Falcke, Release currents of IP_3 receptor channel clusters and concentration profiles, Biophys. J. 86 (2004) 2660–2673.
[28] J.W. Shuai, P. Jung, Optimal ion channel clustering for intracellular calcium signaling, Proc. Natl. Acad. Sci. U. S. A. 100 (2003) 506–510.
[29] J.W. Shuai, P. Jung, Selection of intracellular calcium patterns in a model with clustered Ca^{2+} release channels, Phys. Rev., E 67 (2003) 031905.1–031905.8.
[30] W.H. Press, S.A. Teukolsky, W.T. Vetterling, B.P. Flannery, Numerical Recipes in C, Cambridge University Press, 1992.
[31] T. Kawanishi, L.M. Blank, A.T. Harootunian, M.T. Smith, R.Y. Tsien, Ca^{2+} oscillations induced by hormonal stimulation of individual fura-2-loaded hepatocytes, J. Biol. Chem. 264 (1989) 12859–12866.
[32] A. Neiman, A. Silchenko, V. Anishchenko, L. Schimansky-Geier, Stochastic resonance: noise-enhanced phase coherence, Phys. Rev., E 58 (1998) 7118–7125.
[33] M.G. Rosenblum, A.S. Pikovsky, J. Kurths, Phase synchronization of chaotic oscillators, Phys. Rev. Lett. 76 (1996) 1804–1807.
[34] P. Tass, M.G. Rosenblum, J. Weule, J. Kurths, A.S. Pikovsky, J. Volkmann, A. Schnitzler, H.J. Freund, Detection of n:m phase locking from noisy data: application to magnetoencephalography, Phys. Rev. Lett. 81 (1998) 3291–3294.
[35] G.V. Osipov, A.S. Pikovsky, M.G. Rosenblum, J. Kurths, Phase synchronization effects in a lattice of nonidentical RÖssler oscillators, Phys. Rev., E 55 (1997) 2353–2361.
[36] A.S. Pikovsky, M. Rosenblum, J. Kurths, Phase synchronization of chaotic oscillators by external driving, Physica, D (Amst.) 140 (1997) 219–238.
[37] X. Pei, L. Wilkens, F. Moss, Noise-mediated spike timing precision from aperiodic stimuli in an array of Hodgekin–Huxley-type neurons, Phys. Rev. Lett. 77 (1996) 4679–4682.
[38] M.H. Nathanson, A.D. Burgstahler, Coordination of hormone-induced calcium signals in isolated rat hepatocyte couplets—demonstration with confocal microscopy, Mol. Biol. Cell 3 (1992) 113–121.
[39] L. Combettes, D. Tran, T. Tordjmann, M. Laurent, B. Berthon, M. Claret, Ca^{2+}-mobilizing hormones induce sequentially ordered Ca^{2+} signals in multicellular systems of rat hepatocytes, Biochem. J. 304 (1994) 585–594.